DOI: 10.1002/chem.200401081

Chiral Interactions in Azobenzene Dimers: A Combined Experimental and Theoretical Study

Anna Painelli,*[a] Francesca Terenziani,[a, b] Luigi Angiolini,[c] Tiziana Benelli,[c] and Loris Giorgini[c]

Abstract: To investigate interchromophore interactions in azobenzene polymers, we have undertaken a thorough spectroscopic analysis of the azodye [(*S*)-3-pivaloyloxy-1-(4′-nitro-4-azobenzene)pyrrolidine] by modeling the repeating unit of poly[(*S*)-3-methacryloyloxy-1-(4′-nitro-4-azobenzene)pyrrolidine) and its dimeric derivative whose synthesis is presented here. The analysis of the electronic and Raman spectra of the azodye in several solvents is based on a previously proposed model for polar chromophores in solution. Electronic and CD spectra of the dimeric unit are collected and analyzed within the framework of a new model. On the basis of the information collected from the spectroscopic analysis of the solvated dye, this model accounts for interchromophore interactions in the dimer. The large CD signal measured for the dimer (amounting to about a third of the signal measured for the polymer) suggests the presence of important chiral interactions in the dimeric unit, and is modeled in terms of a right-handed relative orientation of the two chromophores.

Keywords: azo compounds · circular dichroism · Raman spectroscopy · solvatochromism · UV/Vis spectroscopy

Introduction

Donor–acceptor (D–A)-substituted azobenzenes are a well-known family of organic dyes whose color can be tuned by adjusting the strength of the D and/or A end groups.[1] These molecules, which belong to the wider class of D–π-A (or push–pull) chromophores, have been extensively investigated for second-order NLO applications. In this context, dispersed-red 1 is a common reference chromophore.[2] Polymers functionalized with azobenzene side groups (azopolymers) have been synthesized as potentially interesting materials for several applications: a fairly large concentration of chromophores can in fact be loaded into the polymers to obtain films of good optical quality. The properties of the films can be finely tuned by adjusting the chromophore concentration, by changing the D and A substituents in the azo dye, or by altering the nature of the polymeric backbone.[3]

Azodyes undergo a photoinduced *trans–cis* isomerization that is responsible for the intriguing photochromic behavior of azopolymers.[4] In particular, all-optical poling has been demonstrated by shining linearly polarized light on azopolymer films.[5] Even more impressive is the possibility of writing relief gratings over the surface of a film illuminated by interference patterns of linearly polarized laser beams.[6]

Conformational chirality can be optically induced in azopolymer films. Elliptically polarized light induces chirality on amorphous achiral films.[7] Moreover the resulting chiral material can be switched between the two enantiomeric structures by simply alternating irradiation with left and right circularly polarized light.[8] In achiral films of liquid-crystalline azopolymers, circularly polarized light (without a linear component) can induce chirality.[9] In chiral polymers, in which the azodye is grafted onto the polymeric backbone through an enantiomerically pure chiral bridge, the native

[a] Prof. Dr. A. Painelli, Dr. F. Terenziani
Dipartimento di Chimica GIAF and INSTM UdR-Parma
Università di Parma
viale delle Scienze 17/a, 43100 Parma (Italy)
Fax: (+39) 0521-905-556
E-mail: anna.painelli@unipr.it

[b] Dr. F. Terenziani
Synthèse et Electrosynthèse Organiques (CNRS, UMR 6510)
Institut de Chimie
Université de Rennes 1, Campus de Beaulieu
Bât. 10 A, 35042 Rennes Cedex (France)

[c] Prof. Dr. L. Angiolini, Dr. T. Benelli, Dr. L. Giorgini
Dipartimento di Chimica Industriale e dei Materiali and INSTM
UdR-Bologna, Università di Bologna
viale Risorgimento 4, 40136 Bologna (Italy)

Supporting information for this article is available on the WWW under http://www.chemeurj.org/ or from the authors.

polymers show a well-pronounced circular dichroism (CD) signal in the region of the visible absorption of azodyes, demonstrating that the chirality of the bridge induces interchromophoric interactions with a predominant helicity.[10] Successive cycles of irradiation with circularly polarized light with alternating *L* and *R* character force the system into two enantiomeric states with opposite CD spectra.[11] The two enantiomers are temporally and thermally stable, suggesting that circularly polarized light drives chiral azopolymer films into a genuine bistable regime.[12]

Photoinduced chirality, and particularly the observation of a bistable regime in chiral azopolymer films, makes these materials very promising for applications in optical computing and more generally in the optical storage and manipulation of information.[4] However, so far, there is no clear understanding of the mechanism of optically induced chirality or of chiral interactions in azopolymers. It is generally accepted that chirality is induced in these materials as a consequence of chiral interchromophore interactions, but no detailed modeling of these interactions is available. Herein, we address this fundamental problem in a step-by-step procedure. We first concentrate on an isolated chromophore in solution, (*S*)-3-pivaloyloxy-1-(4′-nitro-4-azobenzene)pyrrolidine (**M**, Scheme 1),

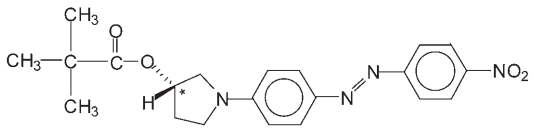

M

Scheme 1. Molecular structure of azodye **M**.

that models the repeating unit of the poly[(*S*)-3-methacryloyloxy-1-(4′-nitro-4-azobenzene)pyrrolidine] polymer. An extensive spectroscopic study of **M** in different solvents leads to the definition of a reliable molecular model for this chromophore. We synthesized the relevant dimeric unit, 2,4-dimethyl-glutaric acid bis(*S*)-3-[1-(4′-nitro-4-azobenzene)]-pyrrolidine ester (**D**, Scheme 2), which corresponds to the

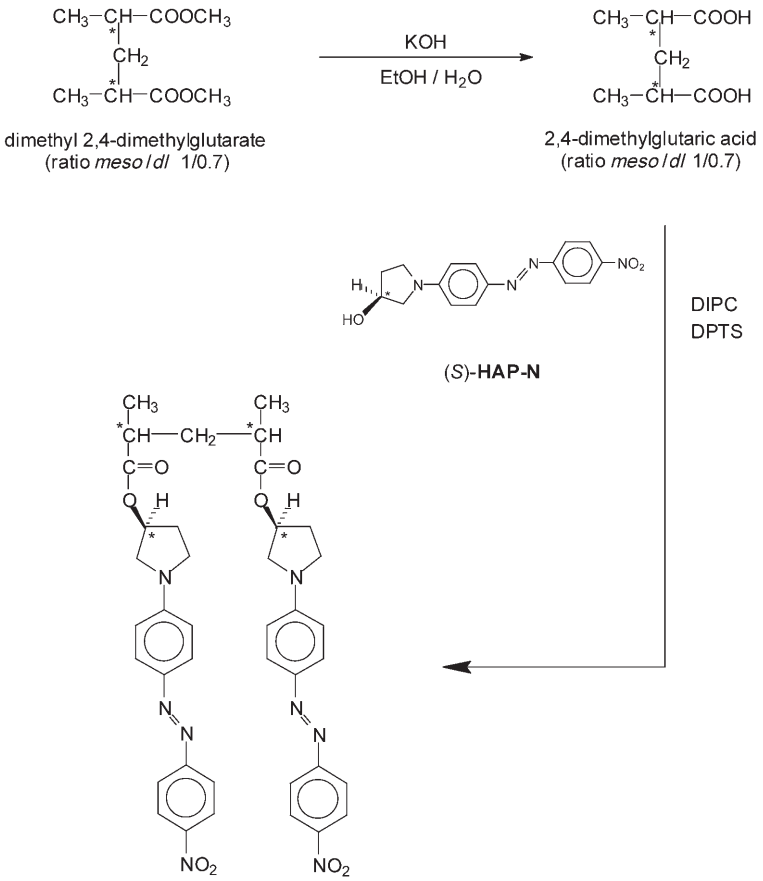

D [ratio *SRSS*/(*SSSS* and *SRRS*) 1/2.1]

Scheme 2. Synthesis of dimeric azodye **D**.

smallest section of the polymer where interchromophore interactions are relevant. Electronic absorption and CD spectra were collected for **D** in several solvents to gain information on interchromophore interactions. Accordingly, we present a model for the dimeric unit and for its spectroscopic behavior in solution that takes advantage of information collected from the spectroscopic analysis of **M**. The resulting picture for interchromophore interactions is the first fundamental step toward the understanding of chiral interactions in azopolymers and of supramolecular interactions in molecular materials, in general.

Results and Discussion

The solvated chromophore: electronic and vibrational spectra: The UV/Vis spectra of **M** (prepared as reported in reference [10a]) in CCl_4, $CHCl_3$, and DMSO are shown in the top panel of Figure 1. The solvents have been selected as representative of nonpolar, slightly polar, and strongly polar media, respectively. The intense absorption in the visible region is characteristic of azodyes and undergoes a well-pronounced red shift with increasing solvent polarity. This *normal* solvatochromism (bathochromism) is typically ob-

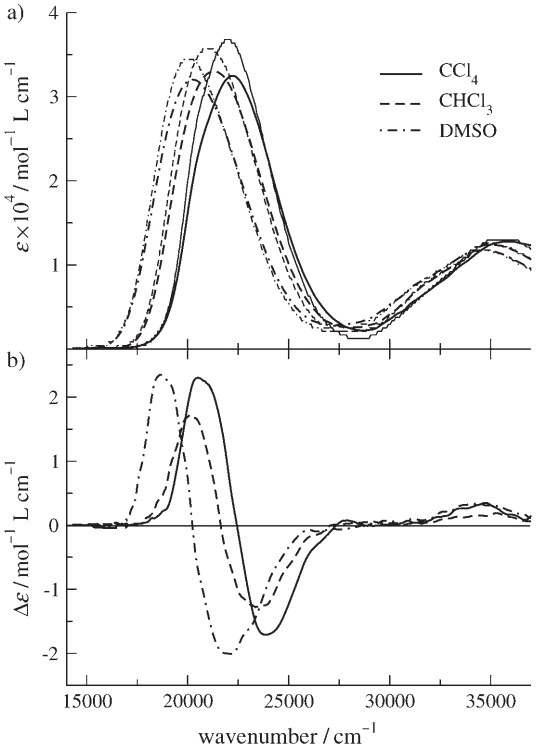

Figure 1. a) Experimental absorption spectra of **D** (heavy lines) and **M** (light lines) dissolved in CCl_4, $CHCl_3$, and DMSO. b) CD spectra of **D** in CCl_4, $CHCl_3$, and DMSO.

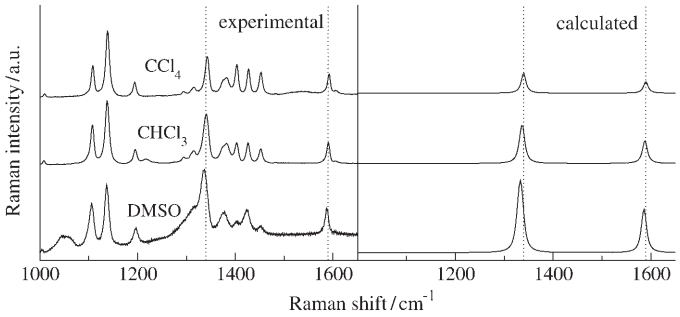

Figure 2. Raman spectra of **M** dissolved in different solvents, with excitation line $\lambda = 647$ nm. Left and right panels show experimental and calculated spectra, respectively. The experimental Raman intensities are rescaled to keep the height of the band at about 1140 cm^{-1} approximately constant. The calculated intensities have the same (arbitrary) units in all the spectra. The vertical dotted lines are drawn as a visual guide.

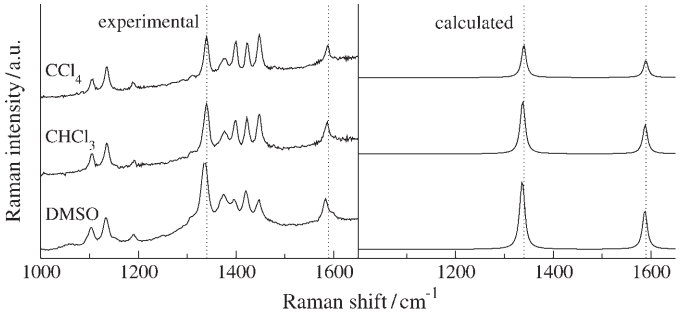

Figure 3. The same as in Figure 2, but with excitation line at $\lambda = 476$ nm.

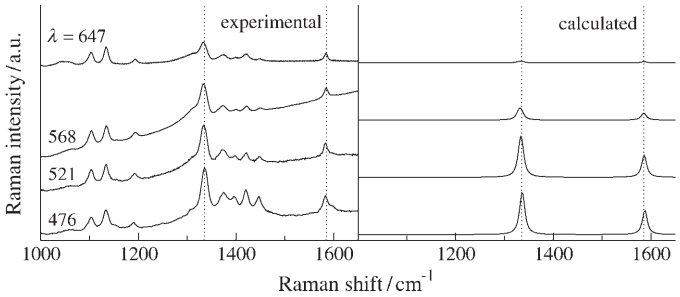

Figure 4. Raman spectra of **M** in DMSO, collected with different excitation lines. Left and right panels show experimental and calculated spectra, respectively. The experimental Raman intensities are rescaled to keep the height of the band at $\approx$1140 cm^{-1} approximately constant. The calculated intensities have the same (arbitrary) units in all the spectra. The vertical dotted lines are drawn as a visual guide.

served for D–π-A chromophores with a neutral ground state, that is, for chromophores whose polarity increases upon photoexcitation.[13]

Azodyes are nonfluorescent. Therefore, to collect additional spectroscopic information, we also measured Raman spectra of **M** in the same solvents with several excitation lines. The complete assignment of the vibrational bands is beyond the scope of this work, here we discuss the Raman spectra just to obtain information about the coupling between electronic and vibrational degrees of freedom, as required for the modeling of the electronic and CD spectra of **M** and **D**.

The left-hand panels of Figure 2 and Figure 3 show Raman spectra of **M** in the three solvents, collected with red ($\lambda = 647$ nm) and blue ($\lambda = 476$ nm) excitation lines, respectively. The red excitation falls, for all solvents, below or just at the lowest energy edge of the absorption band so that the spectra in Figure 2 are nonresonant, or at most preresonant. The blue line corresponds to a resonant excitation for all solvents. The comparison between nonresonant and resonant spectra supports resonant amplification of the group of bands located at about 1340 cm^{-1} and of the band at about 1590 cm^{-1} with respect to other bands, suggesting that these modes have the largest coupling with the electronic degrees of freedom involved in the absorption in the visible region. Indeed, as the solvent polarity increases, the lowest energy band in the group of bands located at about 1400 cm^{-1} becomes more prominent. The dominant role of this band at about 1340 cm^{-1} and of the band at 1590 cm^{-1} is nicely confirmed by data in Figure 4, which shows Raman spectra collected with several excitation lines in DMSO, where all excitation lines are resonant or preresonant. Moreover, as the solvent polarity increases, the two bands at about 1340 and 1590 cm^{-1} undergo an appreciable red-shift of about 7 and 5 cm^{-1}, respectively, while all other bands are unaffected (within 2 cm^{-1}). Spectra collected with the yellow ($\lambda = 568$ nm) and green ($\lambda = 521$ nm) lines in different solvents are reported in the Supporting Information.

Modeling the spectroscopic properties of the isolated chromophore: Electronic solvatochromism of D–π-A chromophores is a very well-known phenomenon with a good coverage in recent literature.[13–17] Its basic physics is simple and is related to the variation of the dipole moment of D–π-A chromophores upon photoexcitation: the ground and excited states are stabilized by differing amounts in polar solvents and the transition energy acquires a large dependence on the solvent polarity.[13] Whereas this simple mechanism describes the basic physics of electronic solvatochromism, it fails to account for some more subtle phenomena, including the dependence of absorption intensities and band shapes on the solvent polarity, or the common observation that the emission bands are narrower than the absorption bands. In recent years, two of the authors have proposed a model for D–π-A chromophores that nicely reproduces their spectroscopic behavior.[18,15] The model describes the electronic structure of the chromophore in terms of two basis states, $|DA\rangle$ and $|D^+A^-\rangle$, corresponding to the neutral and charge-separated (zwitterionic) resonating structures of D–π-A chromophores. The relevant electronic Hamiltonian is given by Equation (1),[20] where $\hat{\rho} = (1-\hat{\sigma}_z)/2$ measures the weight of the zwitterionic state, and $\hat{\sigma}_{x/z}$ is the x/z Pauli matrix. The two basis states mix to give a ground and an excited state.

$$H_{el}^{(M)} = 2z\hat{\rho} - \sqrt{2}t\hat{\sigma}_x \quad (1)$$

The polarity of the chromophore is measured by ρ, the ground state expectation value of $\hat{\rho}$.[20] It depends on $2z$, the energy difference between the two basis states, and on $-\sqrt{2}t$, the matrix element responsible for the mixing of the two states.

To describe the optical spectra of D–π-A chromophores in solution, the model must be extended to account for the coupling of electrons with molecular vibrations and solvation degrees of freedom. As for electron-vibration coupling, we introduce a set of coupled coordinates, Q_i. The two basis states are assigned two harmonic potential energy surfaces with exactly the same frequencies, ω_i, but with displaced minima to induce a linear dependence of $2z$ on the Q_i values. The strength of the coupling of the i-th coordinate is measured by the relevant small polaron binding energy, ε_i, corresponding to the relaxation energy of the $|D^+A^-\rangle$ state along the coordinate.[21,22,24]

Solvation effects are twofold. A polar solute polarizes the electronic clouds of the surrounding solvent molecules and an electric field is generated at the solute site that screens the molecular dipole moment.[21,15,17] The electronic degrees of freedom of the solvent (typically in the ultraviolet region) are faster that the electronic degrees of freedom responsible for the chromophore absorption spectrum in the visible. Therefore, the electronic component of the solvation reaction field does not need to be treated explicitly because it enters the model by a renormalization of the model parameters.[21] Strictly speaking, different molecular parameters then apply to the same chromophore in different solvents. However, the electronic polarization is governed by the refractive index of the solvent, which shows minor variations in common organic solvents, thus justifying the use of solvent-independent molecular parameters.[21]

In polar solvents, a second component of the reaction field appears owing to reorientation of the polar solvent molecules around the polar solute.[21] To describe polar solvation, we introduce an effective solvation coordinate, Q_0, whose coupling to the electronic degrees of freedom is measured by the relaxation energy ε_{or}.[21,18,22] At variance with internal vibrations, the solvation coordinate describes a very slow motion and is best treated in the classical approximation. An equilibrium position for Q_0 is defined for each chromophore in solution and depends in a self-consistent way on the chromophore polarity.[22] However, thermal disorder is responsible for deviations of Q_0 from the equilibrium. A solution of push–pull chromophores in polar solvents can then be described as a collection of chromophores, each one in equilibrium with the local configuration of the surrounding solvent (i.e. with the local Q_0), and the probability of each configuration is weighted by the Boltzmann energy distribution.[22,15] Local fluctuations of the reaction field in polar solvents are therefore responsible for inhomogeneous spectral broadening, which shows up in electronic and vibrational spectra with a broadening of the absorption and nonresonant Raman bands, and with the anomalous dispersion with the excitation line of the Raman frequencies of strongly coupled modes.[22,23]

To describe electronic and vibrational spectra of solvated **M**, a set of molecular parameters must be fixed. Following the same procedure successfully applied to phenol blue,[23,24] we fix $\sqrt{2}t = 1$ eV, as a typical value. To account for the two Raman bands at about 1340 and 1590 cm^{-1}, we introduce two molecular vibrations with reference frequencies $\omega_1 = 1351$ and $\omega_2 = 1597$ cm^{-1}, and small polaron binding energies $\varepsilon_1 = 0.09$ and $\varepsilon_2 = 0.05$ eV. Finally, the energy gap between the zwitterionic and the neutral states is fixed as $2z = 2$ eV. With these molecular parameters fixed (see Table 1), the evolution of electronic and Raman spectra with the solvent polarity is modeled by varying just a single parameter, ε_{or}, the solvent relaxation energy, which vanishes for nonpolar solvents and increases with the solvent polarity ($\varepsilon_{or} = 0$, 0.57, 0.95 eV for CCl_4, $CHCl_3$ and DMSO, respectively).

Visible spectra in Figure 5 are calculated along the same lines as those discussed in reference [15], and by adopting the same intrinsic electronic width, $\Gamma = 2900$ cm^{-1}, for all spectra. The spectra nicely reproduce the evolution of the absorption and emission frequencies as well as the intensities with the solvent polarity. This is a nontrivial result because all molecular parameters are kept fixed, and the solvent effects are accounted for by tuning ε_{or}. In particular, the experimental oscillator strength smoothly increases with increasing solvent polarity. This behavior is reproduced within our model and is understood in terms of a slight increase of the molecular polarity (from $\rho = 0.15$ to 0.20 from CCl_4 to DMSO).[25] The quantitative comparison of absolute intensities fixes the dipole moment of $|D^+A^-\rangle$ to $\mu_0 \approx 20$ D.

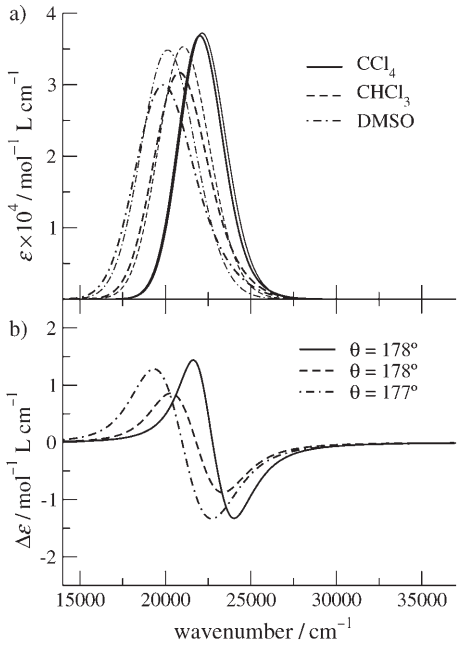

Figure 5. Calculated a) absorption spectra of **D** (heavy lines) and **M** (light lines), and b) circular dichroism spectra of **D** in different solvents.

The same parameters used for electronic spectra were applied to the calculation of Raman spectra shown in the right-hand panels of Figure 2, Figure 3, and Figure 4 (other results are reported in the Supporting Information). Spectra are calculated as described in the literature,[22–24] and by fixing the intrinsic vibrational linewidth as $\gamma = 10\,\mathrm{cm}^{-1}$. The model reproduces the red shift of the Raman bands of the two coupled modes with increasing solvent polarity, as well as the variation of the relative Raman intensities. This is particularly evident for data in Figure 4, which shows Raman spectra collected in DMSO with different excitation lines from preresonant (red excitation) to fully resonant (blue excitation). Figure 2 and Figure 3 show instead spectra collected with a single excitation line (red and blue, respectively), in different solvents. The variations of the intensities are clearly related to the electronic solvatochromism, so that, in both cases, spectra collected in DMSO are more resonant with the chosen excitation line than those in CCl_4.[26] Overall, the agreement between the experimental and the calculated spectra for **M** is very good, giving us confidence in the adopted model and on the estimated molecular parameters.

The dimer: synthesis and characterization: The synthesis of **D** (Scheme 2) starts from commercial dimethyl 2,4-dimethyl-glutarate (ratio *meso*/*dl* 1/0.7), which is converted to 2,4-dimethyl-glutaric acid[27] (ratio *meso*/*dl* 1/0.7), and successively esterified with the azoic alcohol (*S*)-(−)-3-hydroxy-1-(4′-nitro-4-azobenzene)pyrrolidine, (*S*)-HAP-N, prepared as previously reported.[10] The chemical structure was confirmed by ^{1}H NMR, ^{13}C NMR, and FT-IR (see the Experimental Section). Accurate measurements of the optical activity with the sodium D line were hindered by the strong absorption of the azoaromatic chromophore at that wavelength. However, previous data concerning the optical purity of the 4′-unsubstituted pivaloyl or methacryloyl derivatives prepared through a similar synthetic pathway[10,28,29] suggest an enantiomeric excess larger than 95% in those compounds, thus excluding the racemization of the pyrrolidine chiral ring in the synthetic process. We therefore attribute a similar optical purity to the (*S*)-HAP-N residue linked to the side chain of **D**. The H NMR spectra, reported in Figure 6, provide information on the amount of *meso* and racemic stereoisomers of the 2,4-dimethylglutarate residue.

The methylene protons of the glutaric moiety are magnetically equivalent in the racemic isomer and produce a well-defined double triplet centered at $\delta = 1.75$ ppm. In the case of the *meso* isomer, these protons are nonequivalent and appear in the NMR spectrum as two double doublets of doublets centered at $\delta = 2.10$ and 1.45 ppm. From the integrated intensities of these signals, we estimate the molar amount of the *meso* form of the 2,4-dimethyglutarate residue in the sample to be 32%. Analogous values are obtained by analyzing the resonances of the methyl groups in the ^{13}C NMR spectra; the resulting stereoisomeric composition of **D** is well determined (ratio *SRSS*/(*SSSS* + *SRRS*) 1/2.1). The stereoisomeric composition of **D** is by chance similar to that usually obtained for polymethacrylate derivatives prepared by radical polymerization (70% of syndiotactic dyads of the stereogenic centers in the main chain).[10,29,30] In fact, the *SRSS* stereoisomer is the structural model for the isotactic dyad and the *SSSS* and *SRRS* stereoisomers are models for the syndiotactic dyad of poly[(*S*)-MAP-N]. The content of syndiotactic dyads in this polymer amounts to about 72%.[10] Therefore, the study of **D** in its native stereoisomeric composition offers important information on the behavior of the relevant polymer. The synthesis and separation of enantiomerically pure dimers and oligomers is difficult; however, we are currently working on this with the aim of collecting more detailed information on stereochemical interactions in azobenzene polymers.

Electronic absorption and circular dichroism (CD) spectra of **D** in different solvents (see the Experimental Section) are shown in Figure 1. Dimerization barely affects the electronic absorption spectra, except for a small decrease in the intensity. The negligible excitonic effects in absorption spectra of **D** point to weak interchromophore interactions. The sizeable CD signal observed in the visible region instead demonstrates a finite chiral interaction between the chromophores. Specifically, when normalized to the concentration of the chromophoric units, the CD signal measured for **D** is $\approx 1/3$ of the signal measured for the corresponding polymer,[10] suggesting that the CD signal exhibited by the polymer may be attributable to the presence of fairly short chain segments with a well-defined skewness, and does not necessarily imply long-range chiral order.

The dimer: interchromophore interactions from electronic and CD spectra: To describe **D**, we assume that each chro-

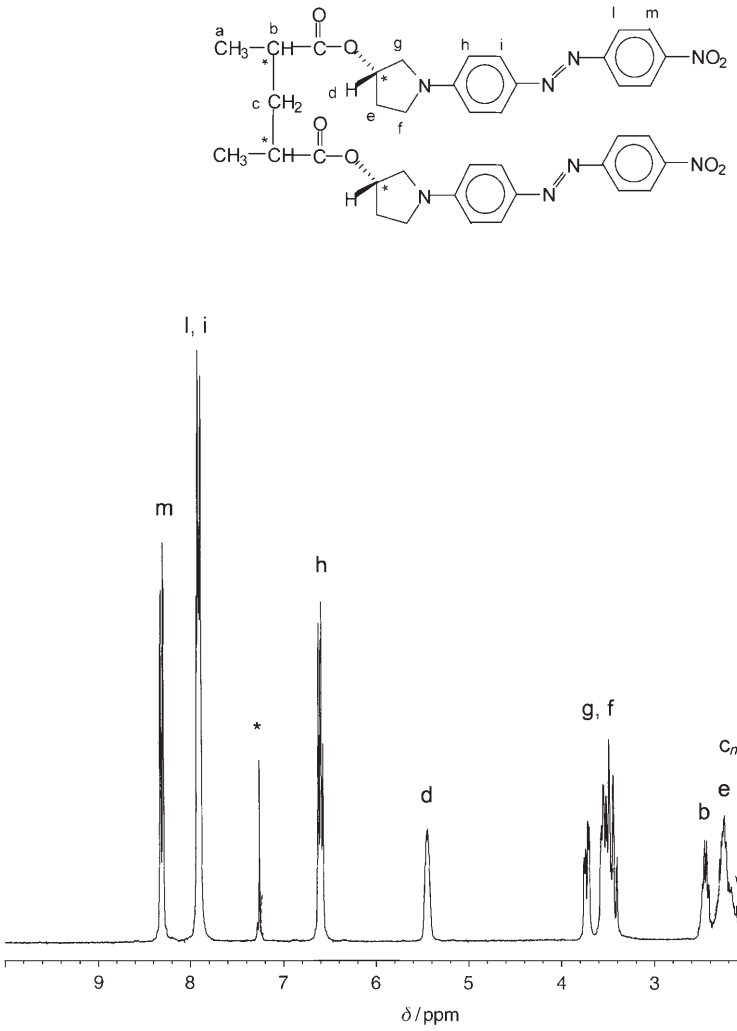

Figure 6. ^{1}H NMR spectra of the azodye **D** in $CDCl_3$. The resonances marked with an asterisk belong to the solvent.

This Hamiltonian must be extended to account for electron-vibration coupling and for solvation effects. For **D**, we only discuss electronic (absorption and CD) spectra so that we can adopt a simplified description of electron–vibration coupling. To describe the Raman spectra of **M** in the section on the solvated chromophore above, we accounted for two coupled modes per chromophore (the two modes with frequency ω_1 and ω_2 in Table 1). However, such a detailed description of the vibrational degrees of freedom is not actually required to model the electronic spectra. Electronic spectra of polar chromophores in solution are fairly broad and structureless, so that accounting for just one effective coupled vibration is most often enough.[15,17,23] In particular, the electronic absorption spectra of **M** in Figure 5, calculated by accounting for both coupled vibrations, is superimposed, at the scale of the figure, with the spectrum calculated by accounting for just the most strongly coupled mode (that with frequency ω_1 in Table 1). Therefore, in the following, we adopt a simplified description for the electron–vibration coupling by only accounting for a single coupled vibration per chromophore. The relevant vibrational Hamiltonian is then represented by Equation (3), where i runs on the two chromophoric sites, and $Q_{1,i}$ and $P_{1,i}$ are the coordinate and conjugated momentum that describe the coupled harmonic oscillator relevant to the i-th chromophore. Finally, ω_1 and ε_1 are the frequency of the oscillator and the corresponding small polaron binding energy, respectively: they are the same for both chromophores, and their values are taken from Table 1.

mophore is surrounded by its own solvation sphere. This approximation is justified by the fairly large interchromophore distance and is supported by the strong similarity of absorption spectra measured for **M** and **D** (Figure 1). Within this approximation, the model parameters extracted from the study of **M** can be transferred to the analysis of **D**. We therefore describe the electronic structure of **D** based on a model recently proposed to describe interacting D-π-A chromophores.[31,32] The relevant Hamiltonian is given by Equation (2), where the first term describes the two chromophores based on the Hamiltonian in Equation (1), with the index i running on the two chromophores.

$$H_{\mathrm{el}} = \sum_{i=1,2} (2z\hat{\rho}_i - \sqrt{2}t\hat{\sigma}_{x,i}) + V\hat{\rho}_1\hat{\rho}_2 \qquad (2)$$

The last term accounts for interchromophore interactions, with V measuring the electrostatic interaction between two zwitterionic, $|D^+A^-\rangle$, chromophores.

Table 1. Molecular parameters fixed for **M** and the three $\varepsilon_{\mathrm{or}}$ corresponding to the three solvents of interest. Units: eV.

							$\varepsilon_{\mathrm{or}}$	
z	$\sqrt{2t}$	ω_1	ε_1	ω_2	ε_2	CCl_4	$CHCl_3$	DMSO
1.0	1.0	0.17	0.09	0.20	0.05	0	0.57	0.95

$$H_{\mathrm{vib}} = \sum_{i=1,2} \frac{1}{2}(\omega_1^2 Q_{1,i}^2 - P_{1,i}^2) - \sqrt{2\varepsilon_1}\omega_1 Q_{1,i}\hat{\rho}_i \qquad (3)$$

Similarly, we model polar solvation by introducing two effective solvation coordinates $Q_{0,i}$, with i running on the two chromophoric sites. The solvation relaxation energy, ε_{or}, relevant to each solvent is taken from Table 1, which results from the spectroscopic analysis of **M**. The two solvation coordinates enter as classical coordinates, the relevant Hamiltonian is given by Equation (4), where the frequency ω_0 assigned to the effective solvation coordinate is irrelevant.[21]

$$H_{solv} = \sum_{i=1,2} \frac{1}{2}\omega_0^2 Q_{0,i}^2 - \sqrt{2\varepsilon_{or}}\omega_0 Q_{0,i}\rho_i \quad (4)$$

The total Hamiltonian $H = H_{el} + H_{vib} + H_{solv}$ can be diagonalized exactly for fixed $Q_{0,1}$, $Q_{0,2}$, to span the distribution of the reaction fields surrounding the two chromophores.

Whereas solvation coordinates are treated as classical variables, vibrational coordinates must be treated quantum mechanically. For fixed $Q_{0,1}$ and $Q_{0,2}$, the total Hamiltonian describes a complex system with coupled electrons and molecular vibrations. Herein, we present results obtained from the direct (nonadiabatic) diagonalization of the Hamiltonian. Specifically, a complete basis for the problem is obtained from the direct product of the electronic basis multiplied by the vibrational basis. As for the electronic basis, the two-states per chromophore lead to four basis states: $|DA,DA\rangle$, $|D^+A^-,DA\rangle$, $|DA,D^+A^-\rangle$, $|D^+A^-,D^+A^-\rangle$. As for the vibrational states, an oscillator must be considered for each chromophore, and an infinite basis set is associated with each oscillator, composed of states with 0, 1, ···, N vibrational quanta. The matrix elements of the total Hamiltonian for fixed $Q_{0,1}$, $Q_{0,2}$, can be easily written on the complete basis and a numerically exact diagonalization of the problem can be obtained by truncating the vibrational basis to a finite N, such that a further increase in N does not affect the results. The dimension of the resulting basis set, $4N^2$, increases rapidly with N. In the present case of weak coupling, $N = 4$ is typically sufficient for the calculation of the optical spectra.

The nonadiabatic diagonalization of the Hamiltonian in Equation (4) goes along the lines already discussed for a single chromophoric unit.[33,34] The resulting eigenstates, $|n\rangle$, with energies E_n, enter the expression for the absorption spectra according to Equation (5),[15] where the sum runs over all the excited states, and $|0\rangle$ represents the ground state.

$$\varepsilon(\tilde{\nu})[\mathrm{L\,mol^{-1}\,cm^{-1}}] = \frac{10\pi L}{3\ln 10\hbar c\varepsilon_0}\frac{1}{\sqrt{2\pi}}\sum_n \tilde{\nu}_{n0}|\langle 0|\hat{\mu}|n\rangle|^2 \exp\left\{-\frac{1}{2}\left[\frac{\tilde{\nu}_{n0}-\tilde{\nu}}{\sigma}\right]^2\right\} \quad (5)$$

L is the Avogadro number, c the speed of light, ε_0 the vacuum permittivity (SI units), and $\tilde{\nu}$ is the wavenumber in cm^{-1}. The dipole moment operator is defined as the vectorial sum of the dipole moments relevant to the isolated chromophores: $\hat{\mu} = \hat{\mu}_1 + \hat{\mu}_2$[32].

The CD spectra are calculated with Equation (6),[35,36]

$$\Delta\varepsilon(\tilde{\nu})[\mathrm{L\,mol^{-1}\,cm^{-1}}] = \frac{80\,L}{3\ln 10\hbar c^2\varepsilon_0}\sum_n \frac{\tilde{\nu}^3\Gamma_{n0}}{(\tilde{\nu}_{n0}^2-\tilde{\nu}^2)^2 + \tilde{\nu}^2\Gamma_{n0}^2}R_{n0} \quad (6)$$

where R_{n0} is defined according to Equation (7):

$$R_{n0} = \frac{(E_n-E_0)}{2\hbar}\vec{R}\cdot(\langle n|\hat{\mu}_1|0\rangle \times \langle 0|\hat{\mu}_2|n\rangle) \quad (7)$$

$\vec{R}$ is the vector that joins the two chromophores. Both absorption and CD spectra calculated for each $Q_{0,1}$, $Q_{0,2}$ are weighted according to a Boltzmann distribution and are then summed to calculate the total spectra that fully account for electron–vibration coupling and for solvation effects, including inhomogeneous broadening from polar solvation.

The geometry of **D**, and more precisely the relative orientation of the chromophores, enters the calculation of the absorption spectra in the definition of the total dipole moment operator, $\hat{\mu}$, the vectorial sum of the dipole moments of each chromophore. Both the orientation and the distance between the chromophores enter the calculation of the CD spectra, through the R_{n0} factor in Equation (7). On the other hand, the geometry of **D** implicitly enters the Hamiltonian through V, in Equation (1), which measures the energy of the electrostatic interactions between the two chromophores in the zwitterionic state. To relate V to the dimer geometry, we model each $|D^+A^-\rangle$ as a rigid segment of length l, with unit positive and negative charges at the two extremes. The two chromophores are attached perpendicularly to the oligomeric chain, modeled as a rigid segment of length R. Based on typical bond lengths, we fix R = 4 Å and l = 10 Å, so that V is fully defined by θ, the dihedral angle between the chromophores (Figure 7). The explicit expression for V is discussed in the Experimental Section.

Figure 8 shows the evolution with the dihedral angle, θ, of the absorption and CD spectra calculated for **D** in CCl_4.

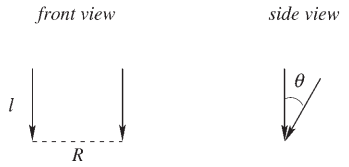

Figure 7. Schematic representation of the considered dimer. Polar molecules are represented by arrows; l is the dipole length, R the interchromophore distance, and θ is the angle formed by the two dipoles.

Only angles between 0 and 180° are shown. Spectra for $-180 < \theta < 0°$ can be obtained easily: upon changing the sign of θ, the absorption spectra are invariant, whereas CD spectra change their sign. The results in Figure 8 were obtained from the complete diagonalization of the electronic and vibrational Hamiltonian; however, the basic physics underlying the spectroscopic behavior of **D** can be understood

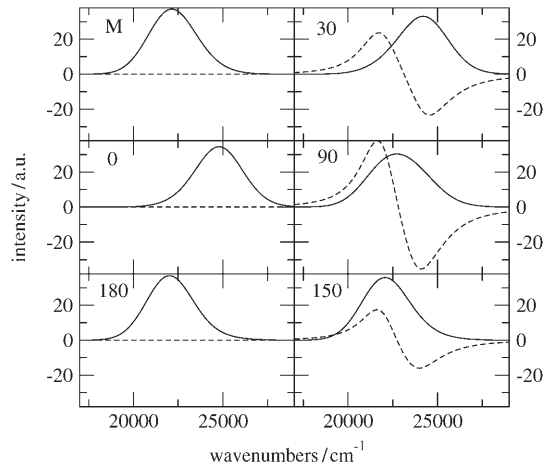

Figure 8. Absorption (——) and CD (-----) spectra calculated for **D** in CCl_4, for θ values shown in each panel. The panel marked with *M* shows the spectra calculated for the isolated **M**. Absorption and CD spectra are reported in arbitrary units, but the corresponding units are the same in all panels.

based on a simple excitonic (or coupled oscillator) model.[36,37,38] The M→M* excitation responsible for the visible absorption in **M** (topmost left panel) corresponds to two excitations in the dimer because each one of the two chromophores can be excited. The two chromophores are equivalent, and it is convenient to combine the two singly excited states as follows: $|E_{\pm}\rangle = (|MM^*\rangle \pm |M^*M\rangle)$, where $|MM\rangle$ represents the dimeric unit and the asterisk marks the excited chromophore within the dimer. Interchromophore interactions split the two states by $2V\rho(1-\rho)$, and, because interchromophore interactions are always repulsive for the adopted geometry, $|E_-\rangle$ corresponds to the lowest excitation.[37,38] For aligned molecules ($\theta = 0$), all oscillator strength resides on $|E_+\rangle$, and the observed spectrum is largely blue-shifted with respect to **M**. For antiparallel orientation ($\theta = 180°$), only E_- is active in absorption: indeed the red-shift with respect to **M** is negligible in this case since the effects of intermolecular interactions are smaller for this orientation. Of course, no CD signal is observed for aligned molecules (either parallel or antiparallel) owing to the lack of chirality. For nonaligned molecules, both E_+ and E_- have a finite intensity for absorption: for $\theta = \pm 90°$ the two transitions have the same intensity, and the resulting absorption spectrum is broad. For $-90 < \theta < 90°$ ($90 < \theta < 270°$) E_+ (E_-) dominates the absorption spectrum: asymmetric absorption spectra are calculated for $\theta = 30°$ and 150°.

A common measure of the strength of the CD spectrum is given in terms of the so-called chiral anisotropy coefficient, *g*, defined as the ratio between the CD signal and the absorbance measured for the same sample at the same frequency (usually the maximum of the CD spectrum).[41] To avoid ambiguities and uncertainties caused by the choice of a specific frequency, we define the integrated *g* factor to be the ratio of the area underlying the absolute value of the CD signal divided by the area underlying the absorption band. Our model for **D** in CCl_4 gives an integrated *g* factor increasing from 0 at $\theta = 0$ to $\theta \approx 154 \times 10^{-5}$ at $\theta = 90°$ and then decreasing again to vanish at $\theta = 180°$. The experimental *g* value for **D** in CCl_4, $g \approx 6.0 \times 10^{-5}$, then imposes θ close to 0 or 180°. Based on the similarity between absorption spectra of **D** and **M**, we safely locate θ close to 180° in CCl_4. Specifically, adopting the model parameters for the chromophore as obtained from the spectroscopic analysis of **M** above, and with the specific choice of the dimer geometry discussed above, the best fit of the CD spectrum in CCl_4 fixes $\theta \approx 178°$. The resulting absorption and CD spectra are shown in Figure 5. The same or very similar angles lead to the best fits of absorption and CD spectra in $CHCl_3$ and DMSO (Figure 5) with the integrated *g* factor $\approx 4.2 \times 10^{-5}$ and $\approx 6.5 \times 10^{-5}$, respectively.

A preliminary discussion of chiral interchromophore interactions in the polymer side chains: The success of the proposed model in the description of absorption and CD spectra of **D** invites us to extend the discussion to the relevant polymeric material. A detailed description of chiral interchromophore interactions in the polymer requires a systematic spectroscopic analysis of trimeric and oligomeric units. Oligomers are challenging in view of both their chemical synthesis and theoretical analysis. However, some preliminary discussion of interchromophore interactions in the macromolecular chain is presented based on information collected for **D**. A crude model for an oligomer is obtained by extending the dimer model to N_M sites (i.e. considering a perfectly ordered chiral structure made up of N_M chromophores): The *i* index in Equation (2) then runs up to N_M and electrostatic interaction, V_{ij}, among all sites are accounted for. Solving the complete electronic and vibrational problem on the $(2N)^{N_M}$ basis is challenging for $N_M > 2$; however, the solution of the electronic Hamiltonian on the 2^{N_M} basis is trivial up to fairly large N_M. The resulting CD spectra cannot give any precise description of experimental spectra, and particularly of band shapes, but they do offer qualitative information on the N_M dependence of the CD signal. Just as an example, if we construct a trimer in DMSO with the same dihedral angle between adjacent chromophores as for the dimer (177°) we get a CD response of approximately the same magnitude as for the dimer but with the *opposite* sign. This result can be easily rationalized: the CD spectra of N_M interacting chromophores roughly corresponds to the sum of the CD spectra resulting from all interactions between pairs of chromophores. In a trimer, we then must sum up two equal contributions from the dimeric interaction between nearest neighbors plus the next-nearest neighbor interaction between two chromophores located 8 Å apart and with a dihedral angle of $\approx 354°$. This last interaction leads to a CD signal that is larger than the sum of the previous two, and has the opposite sign, thus justifying the inversion of the calculated CD signal when going from a dimeric to a trimeric unit. Further increases in N_M give larger and larger CD responses, but still leads to a CD signal with the wrong sign, with respect to the experimental results. Therefore, we must

conclude that the dihedral angle between adjacent chromophores changes on going from **D** to the polymeric system. Experimental spectra for the macromolecular chain can be simulated quite nicely for $\theta \approx 150°$. This estimate, based on an oversimplified description of the polymer, is very rough and represents a preliminary result to be confirmed by further experimental and theoretical studies. However, we underline that a decrease of the dihedral angle when going from a dimeric to an oligomeric unit is expected, based on simple electrostatic arguments, which suggest reduced angles in order to release electrostatic repulsion between non nearest-neighbor chromophores. Overall, within our approach, the experimental negative Cotton effect observed in the CD spectra of **D** is related to a right-handed chiral conformation of the two chromophores. The observation of a Cotton effect with the same sign for the polymer can be similarly explained based on a right-handed conformational structure, such as that relevant to a right-hand helix.

Conclusions

We have presented a combined theoretical and experimental investigation of interchromophore interactions in azobenzene derivatives. The analysis starts from the quantitative description of the chromophoric unit, based on an extensive spectroscopic study of the chromophore in solution. The dimeric unit was then synthesized as an interesting model system to investigate interchromophore interactions in azopolymers. The analysis of CD spectra of **D** in several solvents proved particularly useful in this respect.

The model proposed for optical spectra of **D** is very simple and only accounts for electrostatic interchromophore interactions. Moreover, the adopted geometry is somewhat arbitrary, leading to an oversimplified expression for V (see the Experimental Section). In spite of these limitations, the model nicely reproduces experimental absorption and CD spectra. In particular, in both $CHCl_3$ and DMSO, in agreement with experimental data, we calculated somewhat less intense absorption spectra for **D** than for **M**, as a consequence of 1) the decrease of the chromophore polarity caused by interchromophore interactions, 2) the increased broadening in **D**. The effect is much reduced in CCl_4, leading to some discrepancy with respect to the experimental data. This minor discrepancy could be cured by assigning a small ε_{or} to this nonpolar solvent;[25] however, we do not believe the accuracy of the model is high enough to justify the effort. In any case, our aim is not the detailed fit of the experimental features, nor a precise estimate of microscopic parameters: indeed, the estimated dihedral angles depend on the specific choice of l and R. Instead, our results demonstrate that, starting with an extensive spectroscopic analysis of the solvated **M** chromophore, enough information can be obtained to construct a model for the dimeric unit, **D**. This bottom-up analysis of molecular materials is a first step in the understanding of interchromophore interactions. Specifically, we demonstrate here that both electronic and CD spectra of **D** can be understood in terms of classical electrostatic interactions, based on a realistic description of the **D** geometry.

The CD signal in our model is attributed to the intrinsically chiral interaction between the two chromophoric units for any dihedral angle other than 0 or 180°. The presence of a chiral C center in the side chain is instrumental in favoring the chiral orientation of the chromophores, but, by itself, it is irrelevant to the spectroscopic behavior in the visible region. In this respect, our model shares the same physics with the standard excitonic picture that is usually adopted to describe CD spectra of interacting chromophores.[36,39,40] However, a major difference must be noted. In fact, the electrostatic interchromophore interactions are modeled in the electric dipole approximation in the standard picture. This approximation, strictly valid only in the long-distance regime ($l \ll R$), describes each chromophore as an electric dipole: it corresponds to repulsive/attractive interactions for parallel/antiparallel molecules, and predicts vanishing interactions for perpendicularly oriented chromophores. In our more realistic picture, where the two molecules are anchored through their D site to the rigid polymeric backbone (Figure 7) interchromophore interactions are always finite and repulsive, having their maximum (minimum) value for parallel (antiparallel) molecules. This has, of course, important spectroscopic consequences that are most evident in CD spectra: in our geometry, the CD spectrum only vanishes for parallel or antiparallel chromophores, whereas in the standard model the CD signal vanishes for parallel, antiparallel, and perpendicular chromophores. The vanishing of the CD signal for parallel (or antiparallel) chromophores is trivially related to the lack of chirality in both models. Structures with perpendicular chromophores stay chiral unless the two chromophores are anchored in the middle, which is always the case for point-dipole molecules. Indeed, in the dipole approximation, perpendicular chromophores do not interact and no CD signal is expected in any case.

Our model for CD spectra fully accounts for the coupling of electronic degrees of freedom with vibrational and solvation degrees of freedom. This allows us to discuss CD and absorption spectra on the same footing and gives information not only on the amplitude of the CD signal, but also on the band-shape of the CD spectra. In particular, coupling to slow degrees of freedom (including internal vibrations and polar solvation coordinates) is responsible for the observation of broad absorption and CD spectra. In this respect, we underline that the amount of the exciton splitting ($E_+ - E_-$) cannot be directly extracted from the energy difference between the positive and negative CD peaks in the case of broad spectra. CD spectra are, in fact, the difference of spectra relevant to the E_+ and E_- absorption. In the case of broad spectra, that is, when $E_+ - E_-$ is smaller than the bandwidth, the apparent exciton splitting, obtained from the frequency difference between the positive and negative CD peaks, measures the amount of broadening and not the true splitting. A reliable estimate of the exciton splitting can only be obtained via a detailed fit of both absorption and CD spectra.

Experimental Section

Synthesis of model compound M: This was synthesized as previously reported.[10]

Synthesis of D: An excess of KOH in water (4.8 g, 5 mL) was added to a solution of dimethyl 2,4-dimethylglutarate (Aldrich, ratio *meso*/*dl* 1/0.7) in ethanol (7.41 mmol, 9.5 mL), and the mixture was kept under reflux for 4 h. The solvent was eliminated under reduced pressure and the resulting white solid was dissolved in water. The solution was acidified (pH 1) with concentrated aqueous HCl, and the precipitated material was filtered, dissolved in diethyl ether, and dried with Na_2SO_4. The aqueous solution was repeatedly washed with ether, and the organic phases were collected and dried. The solvent was evaporated, and the pure product (ratio *meso*/*dl* 1/0.7) was immediately used for the following reaction. The diacidic derivative (0.622 mmol) was dissolved in dry CH_2Cl_2 under a nitrogen atmosphere with the azoic alcohol (*S*)-(−)-3-hydroxy-1-(4′-nitro-4-azobenzene)-pyrrolidine [(*S*)-HAP-N, 2.47 mmol], prepared as previously reported.[10] 4-(Dimethylamino)pyridinium 4-toluenesulfonate (DPTS, 1.24 mmol) and 1,3-diisopropylcarbodiimide (DIPC, 1.60 mmol) were added to the solution, and the mixture was stirred for five days at room temperature. The product was purified by column chromatography (SiO_2, $CHCl_3$) followed by crystallization in hot toluene (yield 29%). M.p. 209–211 °C; FT-IR: $\tilde{\nu}$ = 3068 (ν_{CH}, arom.), 2982 and 2949 (ν_{CH}, aliph.), 1733 (ν_{CO}, ester), 1605 and 1516 ($\nu_{C=C}$, arom.), 1140 (ν_{C-O}), 861 and 823 (δ_{CH} 1,4-disubst. arom. ring) cm^{-1}; ^1H NMR: δ = 8.35 (dd, 4H, arom 3′-H), 7.90 (m, 8H, arom *metha* to amino group and 2′-H), 6.60 (dd, 4H, arom *ortho* to amino group), 5.45 (m, 2H, 3-CH), 3.80–3.35 (m, 8H, 2- and 5-CH_2), 2.45 (m, 2H, backbone CH), 2.25 (m, 4H, 4-CH_2), 2.10 and 1.45 (2 ddd, 2H, backbone CH_2 *meso* form), 1.75 (2t, 2H, backbone CH_2 racemic form), 1.15 (d, 6H, CH_3 *meso* form), 1.10 ppm (d, 6H, CH_3 racemic form); ^{13}C NMR: δ = 176.4 (CO), 156.5 (arom C-NO_2), 151.1, 148.1, 144.7 (arom C-N=N-C and C-NCH_2), 126.9, 125.4, 123.3 (arom 3′-C, 2′-C and 3-C), 112.4 (arom 2-C), 74.1 (CH-O), 54.3 (CH-CH_2-N), 46.5 (CH_2-CH_2-N), 38.0 (main chain CH_2-CH), 31.8 (CH_2-CH_2-N), 18.4 (CH_3 racemic form), 18.0 ppm (CH_3 *meso* form).

General procedures: ^1H and ^{13}C NMR spectra were obtained at room temperature in 5–10% $CDCl_3$ solutions with a Varian NMR Gemini 300 spectrometer. Chemical shifts are given with respect to tetramethylsilane (TMS) as the internal reference. ^1H NMR spectra were recorded at 300 MHz with the following experimental conditions: 24000 data points, 4.5 kHz spectral width, 2.6 s acquisition time, 64 transients. ^{13}C NMR spectra were recorded at 75.5 MHz, under full proton decoupling, with the following experimental conditions: 24000 data points, 20 kHz spectral width, 0.6 s acquisition time, 64000 transients. UV/Vis absorption spectra of $CHCl_3$, CCl_4, and DMSO solutions were recorded at 25 °C in the 700–250 nm spectral region with a Perkin-Elmer Lambda 19 spectrophotometer. The cell path length was 0.1 cm. Concentrations of azobenzene chromophore of $\approx 3\times10^{-4}$ mol L^{-1} were used. CD spectra were recorded at 25 °C on a Jasco 810A dichrograph with the same path lengths and solution concentrations as for UV measurements. $\Delta\varepsilon$ values, expressed as $L\,mol^{-1}\,cm^{-1}$, were calculated with Equation (8), where the molar ellipticity $[\theta]$ in $deg\,cm^2\,dmol^{-1}$ refers to one azobenzene chromophore.

$$\Delta\varepsilon = [\theta]/3300 \tag{8}$$

Raman spectra were collected with a Renishow System-1000 Raman microscope, equipped with a Kr laser. The spectral resolution was about 1 cm^{-1}. The following excitation lines were used: 647 nm (red), 568 nm (yellow), 521 nm (green), 476 nm (blue). Spectra obtained with the 568 nm and the 521 nm excitation lines for the solutions in CCl_4, $CHCl_3$, and DMSO are reported in the Supporting Information.

Modeling electrostatic interactions: V represents the electrostatic interaction between two zwitterionic chromophores. Each zwitterionic chromophore was modeled in terms of a pair of unit positive and negative charges at the two extremes of a rigid rope of length l = 10 Å. The two chromophores are perpendicularly attached to the polymeric backbone at a distance of R = 4 Å (Figure 7) and define a dihedral angle θ. Based on this simplified picture for the **D** geometry, V can be calculated by means of Equation (9), where ε_0 is the vacuum dielectric permittivity, and n^2, the squared refractive index of the solvent, accounts for the dielectric screening of electrostatic interactions at optical frequencies.

$$V = \frac{e^2}{4\pi\varepsilon_0 n^2}\left(\frac{1}{R} + \frac{1}{\sqrt{R^2 + 4l^2\sin^2(\theta/2)}} - \frac{2}{\sqrt{l^2 + R^2}}\right) \tag{9}$$

Modeling the screening of electrostatic interactions caused by the solvent is nontrivial, and deserves some discussion. Interchromophore interactions and their screening in solution haven been extensively covered in recent literature; however, most often with reference to centrosymmetric chromophores or to molecules with no permanent dipole moment.[42] In this case, the only relevant electrostatic interactions involve transition dipole moments and should therefore be screened by the dielectric constant at optical frequencies, that is, by the squared refractive index. The problem is more complex in the case of polar chromophores: electrostatic interactions in the ground state involve static charge distributions and should be screened by the static dielectric constant, whereas transient interactions involving either transition or excited state dipole moments should be screened by the squared refractive index. The electrostatic interaction V in Equation (1) enters into the definition of the ground-state chromophore polarity,[32] and in this respect it should account for the static dielectric screening. But the very same quantity also enters the definition of the exciton splitting[32] where the dielectric constant at optical frequencies should play a role. Certainly, there is no ambiguity with respect to in nonpolar solvents, where the static dielectric constant is virtually equal to the squared refractive index. In contrast, the difference is large in strongly polar solvents. For example, in DMSO the static dielectric screening is about 10 times larger than the screening at optical frequencies. To the best of our knowledge, a general solution to this interesting problem is lacking. For the specific system we are discussing in this paper, we take advantage of the comparatively small value of the ground-state dipole moment of **M** and then adopt the same screening model for interchromophore interactions as is usually adopted for nonpolar chromophores, or, in other words, we screen V in Equation (1) by the squared refractive index of the solvent. We can appreciate the quality of this approximation by comparing the ground-state polarity calculated for the chromophores in **D** in the hypothesis of optical or static dielectric screening for interchromophore interactions. In CCl_4, the two screenings are virtually identical and lead to the same ground-state polarity $\rho\approx0.16$. In $CHCl_3$, static screening leads to $\rho\approx0.17$, to be compared with a value of 0.16 obtained in the adopted approximation. By the way, the largest difference was found in DMSO, with ρ = 0.20 and 0.18 for static and optical screening, respectively. In any case, the two results differ by no more than 10%, well within the uncertainties of the proposed model.

Acknowledgements

A.P. is grateful to Aldo Brillante for useful correspondence on CD spectra. F.T. acknowledges support by a Marie Curie Intra-European Fellowship within the 6th European Community Framework Programme. Financial support by MIUR (through FIRB 2001 and PRIN 2004) and INSTM is gratefully acknowledged.

[1] Proceedings of the Symposium on Azobenzene-Containing Materials, Boston, MA, **1998** (Ed.: A. Natansohn), Macromolecular Symposia **1999**, *137*, 1–165.
[2] D. R. Kanis, M. A. Ratner, T. J. Marks, *Chem. Rev.* **1994**, *94*, 195.
[3] a) Z. Sekkat, W. Knoll, *Photoreactive organic thin films*, Amsterdam Academic Press, Amsterdam **2002**; b) O. Nuyken, C. Scherer, A. R. Brenner, U. Dahn, R. Gärtner, S. Kaiser-Röhrich, R. Kollefrath, P. Matusche, B. Voit, *Prog. Polym. Sci.* **1997**, *22*, 93–183; c) S. K. Yesodha, C. K. Sadashiva Pilai, N. Tsutsumi, *Prog. Polym. Sci.* **2004**, *29*, 45–74.
[4] J. A. Delaire, K. Nakatani, *Chem. Rev.* **2000**, *100*, 1817–1845.

[5] F. Charra, F. Devaux, J.-M. Nunzi, P. Raimond, *Phys. Rev. Lett.* **1992**, *68*, 2440–2443.
[6] a) P. Rochon, E. Batalla, A. Natansohn, *Appl. Phys. Lett.* **1995**, *66*, 136; b) D.-Y. Kim, L. Li, J. Kumar, S. K. Tripathy, *Appl. Phys. Lett.* **1995**, *66*, 1166.
[7] M.-J. Kim, B.-G. Shin, J.-J. Kim, D.-Y. Kim, *J. Am. Chem. Soc.* **2002**, *124*, 3504–3505.
[8] G. Iftime, F. L. Labarthet, A. Natansohn, P. Rochon, *J. Am. Chem. Soc.* **2000**, *122*, 12646–12650.
[9] a) L. Nikolova, T. Todorov, M. Ivanov, F. Andruzzi, S. Hvilsted, P. S. Ramanujam, *Opt. Mater.* **1997**, *8*, 255–258; b) I. Nayadenova, L. Nikolova, P. S. Ramanujam, S. Hvilsted, *J. Opt. A* **1999**, *1*, 438–441.
[10] a) L. Angiolini, D. Caretti, L. Giorgini, E. Salatelli, *J. Polym. Sci.* Part A: *Polym. Chem*. **1999**, 37, 3257; b) L. Angiolini, L. Giorgini, E. Salatelli, *e-Polymers* **2003**, *37*.
[11] L. Angiolini, R. Bozio, L. Giorgini, D. Pedron, G. Turco, A. Daurú, *Chem. Eur. J.* **2002**, *8*, 4241–4247.
[12] a) L. Angiolini, T. Benelli, R. Bozio, A. Daurú, L. Giorgini, D. Pedron, *Synth. Met.* **2003**, *139*, 743–746; b) L. Angiolini, R. Bozio, L. Giorgini, D. Pedron, *Synth. Met.* **2003**, *138*, 375–378.
[13] C. Reichardt, *Chem. Rev.* **1994**, *94*, 2319.
[14] M. L. Horng, J. A. Gardecki, A. Papazyan, M. Maroncelli, *J. Phys. Chem.* **1995**, *99*, 17311.
[15] B. Boldrini, E. Cavalli, A. Painelli, F. Terenziani, *J. Phys. Chem. A* **2002**, *106* , 6286–6294; and references therein.
[16] D. Laage, W. H. Thompson, M. Blanchard-Desce, J. T. Hynes, *J. Phys. Chem. A* **2003**, *107*, 6032–6046.
[17] F. Terenziani, A. Painelli, A. Girlando, R. M. Metzger, *J. Phys. Chem. B* **2004**, *108*, 10743–10750.
[18] A. Painelli, F. Terenziani, *Chem. Phys. Lett.* **1999**, *312*, 211.
[19] R. S. Mulliken, *J. Am. Chem. Soc.* **1952**, *74*, 811.
[20] A. Painelli, *Chem. Phys. Lett.* **1998**, *285*, 352.
[21] A. Painelli, *Chem. Phys.* **1999**, *245*, 185–197.
[22] A. Painelli, F. Terenziani, *J. Phys. Chem. A* **2000**, *104*, 11041.
[23] F. Terenziani, A. Painelli, D. Comoretto, *J. Phys. Chem. A* **2000**, *104*, 11049.
[24] A. Painelli, F. Terenziani, *Synth. Met.* **2001** *116* 135–138.
[25] The absorption spectrum calculated in CCl_4 is somewhat narrower than the experimental spectrum. This small discrepancy can be easily accounted for by assigning a small ε_{or} to this solvent. Whereas a small but finite ε_{or} in CCl_4 can be justified as accounting for quadrupolar contributions to the orientational reaction field,[15] we feel that this correction is not really required for the scope of the present work.
[26] We underline that the strength of the coupling between electronic and vibrational degrees of freedom is much lower for **M** than for phenol blue. At the same time, **M** is less polar, and hence less polarizable than phenol blue. Both facts concur to reduce the effects of coupling in vibrational spectra. In particular, the inhomogeneous broadening that strongly affects Raman spectra of phenol blue[23,24] is barely appreciable in the present spectra.
[27] H. Achenbach, W. Karl, *Chem. Ber.* **1975**, *108*, 759–771.
[28] L. Angiolini, D. Caretti, C. Carlini, L. Giorgini, E. Salatelli, *Macromol. Chem. Phys.* **1999** *200*, 390.
[29] a) L. Angiolini, D. Caretti, L. Giorgini, E. Salatelli, A. Altomare, C. Carlini, R. Solaro, *Polymer* **1998** *39*, 6621; b) L. Angiolini, D. Caretti, L. Giorgini, E. Salatelli, A. Altomare, C. Carlini, R. Solaro, *Polymer* **2000**, *41*, 4767.
[30] a) I. R. Peat, W. F. Reynolds, *Tetrahedron Lett.* **1972**, *13*, 1359; b) E. F. McCord, W. L. Anton, L. Wilczek, S. D. Ittel, L. T. J. Nelson, K. D. Raffael, *Macromol. Symp.* **1994**, *86*, 47; c) L. Angiolini, D. Caretti, L. Giorgini, E. Salatelli, *Polymer*, **2001** *42*, 4005; d) L. Angiolini, D. Caretti, L. Giorgini, E. Salatelli, *e-Polym. e-Polymers* **2001**, *21*.
[31] A. Painelli, F. Terenziani, *J. Am. Chem. Soc.* **2003**, *125* 5624–5625.
[32] F. Terenziani, A. Painelli, *Phys. Rev. B* **2003**, *68*, 165405 (1–13).
[33] L. Del Freo, A. Painelli, *Chem. Phys. Lett.* **2001**, *338*, 208.
[34] L. Del Freo, F. Terenziani, A. Painelli, *J. Chem. Phys.* **2002**, *116*, 755–761.
[35] E. U. Condon, *Rev. Mod. Phys.* **1937**, *9*, 432–456.
[36] D. P. Craig, T. Thirunamachandran, *Molecular Quantum Electrodynamics*, Academic press, London **1984**, Chapt. 8.
[37] V. M. Agranovich and M. D. Galanin, *Electronic Excitation Energy Transfer in Condensed Matter* North-Holland, Amsterdam, **1982**.
[38] J. Knoester, in *Organic Nanostructures: Science and Applications* (Eds.: V. M. Agranovich, G. C. La Rocca), IOS Press, Amsterdam **2002**, p. 149, and references therein.
[39] A. Rodger, B. Nordén, *Circular Dichroism and Linear Dichroism*, Oxford University Press, Oxford **1997**, Chapts. 5 and 7.
[40] S. F. Mason, *Molecular Optical Activity and the Chiral Discrimination*, Cambridge University Press, Cambridge **1982**, Chapt. 3.
[41] N. Berova, K. Nakanishi, R. W. Woody, *Circular dichroism, principles and applications*, Wiley-VCH Inc., New York, **2000**.
[42] G. D. Scholes, *Annu. Rev. Phys. Chem.* **2003**, *54*, 87.

Received: October 25, 2004
Revised: May 13, 2005
Published online: July 29, 2005

